Reversionary rotation of actuated particles for microfluidic near-surface mixing

Reversionary rotation of actuated particles for microfluidic near-surface mixing

Roy J. S. Derks,[1] Arjan J. H. Frijns,[1] Menno W. J. Prins,[2,3] and Andreas Dietzel[1,4,a)]
[1]*Department of Mechanical Engineering, Eindhoven University of Technology, PO Box 513, 5600 MB Eindhoven, The Netherlands*
[2]*Department of Applied Physics, Eindhoven University of Technology, PO Box 513, 5600 MB Eindhoven, The Netherlands*
[3]*Philips Research Europe, High Tech Campus 4, 5656 AE Eindhoven, The Netherlands*
[4]*Holst Centre, High Tech Campus 31, PO Box 8550, 5605 KN Eindhoven, The Netherlands*

(Received 4 May 2011; accepted 23 June 2011; published online 13 July 2011)

The off-axis motion of particles actuated by axial magnetic or gravitational forces is studied in fluidic channels. Single actuated superparamagnetic micro-particles starting from channel walls travel towards the channel center and show unforeseen reversionary rotation phenomena. Different stages of co- and counter-rotation are observed in both micro- and macro-scale experiments and are analyzed by means of numerical fluid-dynamics models. The related microfluidic near-surface mixing performance of the rotating actuated particles is discussed. © *2011 American Institute of Physics*. [doi:10.1063/1.3610564]

Miniaturization is a key trend in analytical chemistry devices, helping systems to become faster, more sensitive and cheaper.[1] In microfluidic systems, challenges are faced when fluids are forced into motion: Large fluid-to-wall contact-areas create large pressure drops over small distances.[2,3] Furthermore, the absence of turbulence obstructs efficient mixing and molecular diffusion is too slow for most processes.[4] Fluid elements near no-slip boundaries experience a higher residence time compared to elements in the center of a fluid volume. This hinders fast and efficient reaction kinetics due to depletion zones, which can be tens of micrometers thick for DNA or proteins at typical pico-molar concentrations.[5] Therefore, it is crucial to pump and mix at the same time, everywhere in the fluid volume. The integration of both functionalities on chip is challenging.[3,6] In previous studies, we have demonstrated that magnetic particles can be effectively used as fluid drivers in high surface area microsystems.[2,7] In this paper, we focus on the off-axis motion of particles. We start analyzing the hydrodynamic focusing of off-axis particles in a laminar flow. Focusing mechanisms of particles in a passive flow and particles forced by external magnetic fields are compared by simulations and experiments. Effects of particle co-rotation (passive particles) and counter-rotation (actuated particles) are analyzed experimentally in microchannel systems. The rotational degree of freedom of actuated particles is discussed in view of the enhancement of near-surface mixing, where the particles act as integrated fluid drivers and mixing agents at the same time.

If a particle is carried along in a pressure driven Poiseuille flow, the particle tends to focus towards the channel center. This so-called tubular pinch effect has been described in many studies for particles that passively follow the flow where inertial forces can be neglected.[8–10] Here, the particle is exposed to only viscous forces and is density matched with the surrounding fluid. The particle will lag behind the average fluid flow ($v/v_{f,avg} < 1$) and experiences different fluid velocities at its wall-side oriented half-sphere surface (lower velocity) and at its channel-axis oriented half-sphere surface (higher velocity). The lower velocity will induce a higher pressure and vice versa according to Bernoulli's law, which forces the particle to levitate from the wall and to focus itself towards the channel center.[9] Additionally, the drag forces in opposing directions impose a moment on the particle, which starts to rotate as if rolling over the channel wall, further amplifying the velocity gradients and the focusing effect.[11,12] The exact particle trajectory is, however, very difficult to predict due to the many parameters of influence.[13,14] The axial particle velocity v, the rotational velocity ω, the average surrounding fluid velocity v_f, and the channel confinement expressed as R/r affect the particle focusing, where R is the channel radius and r is the particle radius. For a 2D case, the Kutta-Joukowski lift theorem calculates the lift or focus force according to: $F_{focus} = 4\rho\pi^2 r^3 v\omega$.[15] In our case of a 3D particle being highly confined by the channel, this equation will not give an accurate prediction; however, it can nevertheless be used to qualitatively reconstruct the trajectory shape. A full 3D CFD model has been developed in COMSOL MULTIPHYSICS (Ref. 16) in order to calculate the axial particle translation velocity v and rotational velocity ω as function of its radial position in a Poiseuille flow. A microchannel with no-slip boundaries with radius R and length L is assumed to be filled with water (density $\rho = 1000$ kg/m^3 and viscosity $\eta = 1$ mPa·s). No external actuation force acts on the particle but an external pressure drop of $\Delta p = 0.25$ Pa is applied over the fluid in the channel ($L = 5$ mm). The fluid flow is laminar (Re $\ll 1$) and Brownian motion can be neglected. The focusing force F_{focus} is calculated with the results of the simulation that is performed over time. As shown in Figure 1(a) (dashed line), a passive particle starting from a wall (at $x = R - r$) will levitate from the wall immediately as the radial velocity gradient (x-direction) is locally very high. Approaching the center, the focusing force disappears resulting in an "L-shaped" focusing curve.

a)Author to whom correspondence should be addressed. Electronic mail: a.h.dietzel@tue.nl

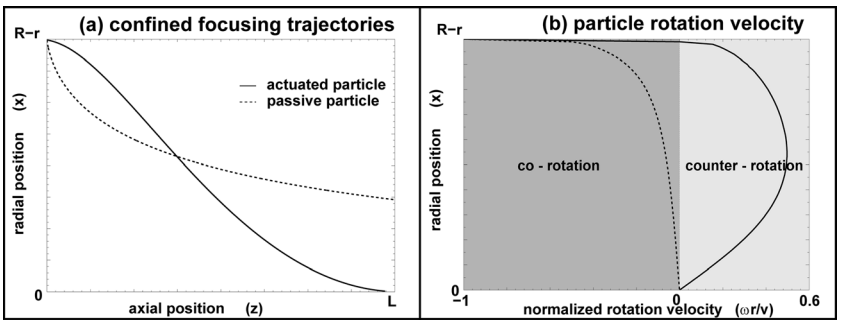

FIG. 1. Computed trajectories (a) and rotation (b) for particles in a fluidic channel. Trajectories are shown for a passive particle in a pressure driven flow (solid line) and for a particle that is actively actuated by an externally applied force in an initially quiescent fluid (dashed line). The particles start at the channel wall and move toward the channel center. For the passive particle, the steepest focusing is observed near the channel wall. For the actuated particle, the steepest focusing is observed halfway the wall and the center. For every radial position, the normalized rotation $(\omega r)/v$ is plotted (b). Close to the wall $(R\text{-}r)$, the passive and actuated particle roll over the surface with $(\omega r)/v = -1$, which we call co-rotation. The passive particle steeply loses its rotation while moving away from the wall. The actuated particle switches from co-rotation to counter-rotation, with a maximum counter-rotation of $(\omega r)/v = +0.5$ halfway the wall and the center. At the channel center, the rotation vanishes $(\omega r)/v = 0$.

In microchannel experiments carried out under active magnetic forcing of the particles,[7] focusing effects were also observed but evidently differ from the case of passive particles in a pressure driven flow. In these studies, the channel was filled with a solution of superparamagnetic particles of 20 μm in diameter (Spherotech, USA), which experienced an individual particle force of $F_m = 20$ fN along the channel under the action of the applied magnetic field ($\nabla B^2 \approx 0.2$ T^2/m). Four different stages can be distinguished for an actuated particle, as shown in Figure 2 (top panels). Very close to the wall, the particle rotates (similar to a passive particle) as if it rolls over the surface, shown in panel (a). As the actuated particle moves faster than the fluid, this rotation prevents the fluid from reaching a high velocity across the half-sphere surface facing the channel axis and the particle stays virtually attached to the wall, until another effect upsets this situation. At the macro-scale, one could think of a slightest onset of turbulence.[9,17] In our case of laminar flows ($Re \approx 10^{-4}$), the disturbance may have come from surface roughness (wall or particle) or particle anisotropy (shape or magnetization). Panel (b) shows a particle that has finally detached from the wall, accompanied by reduced particle rotation and starts to slip. While further separating from the wall, the particle completely reverses its rotation direction as shown in panel (c). Approaching the channel axis, the focusing force and counter-rotation slowly disappears and the particle finds its equilibrium at the channel center (d). Despite the clear transitions shown in Figure 2 (top panels), repeated experiments showed that an exact reconstruction of the focusing trajectory on the micro-scale was very difficult. Therefore, a macro-scaled experiment was performed where a particle starting from the channel wall was driven by gravitation. A plastic tube of 1 m in length and 15 mm in diameter was placed vertically and was closed at the bottom to reflect infinite channel length conditions. Stainless steel particles are used with a diameter of 5 mm and a density of 7860 kg/m^3. To meet the low Reynolds number regime (Re $\ll$ 1) as in the magnetic particle experiments, the tube was filled with viscous oil (SAE 80W90, Comma, United Kingdom, $\rho = 887$ kg/m^3, $\eta = 200$ mPa·s at 20°C). As shown in Figure 2(e) (bottom panel), these experiments typically reveal an s-shaped focusing trajectory.

To reconstruct the focusing trajectory of an actuated particle, the COMSOL MULTIPHYSICS (Ref. 16) model was used again, where the particle experiences an actuation force F_m in the axial direction and the external pressure component Δp has been removed. The computed curve shown in Figure 1 (solid line) does not concur with the case of a passive particle (dotted line), but shows the more complex "S-shaped" trajectory, similar to our experimental observations. The above analyses allow to reason that these two focusing phenomena are of different nature. Remarkably, only few publications have been found indicating a reversionary rotation phenomenon on the macro-scale, but without a satisfying explanation.[12,17] For better understanding, the particle rotation velocities that have been calculated with the simulation model are plotted as a function of the radial position of the particle in Figure 1(b), for both a passive particle (dashed line) and an actuated particle (solid line). The particle rotation is normalized to its translation velocity, as the simulation results show that the particle rotation ω is proportional to its translation velocity v. On the position virtually attached to the wall $(x = R - r)$, both particles roll over the surface

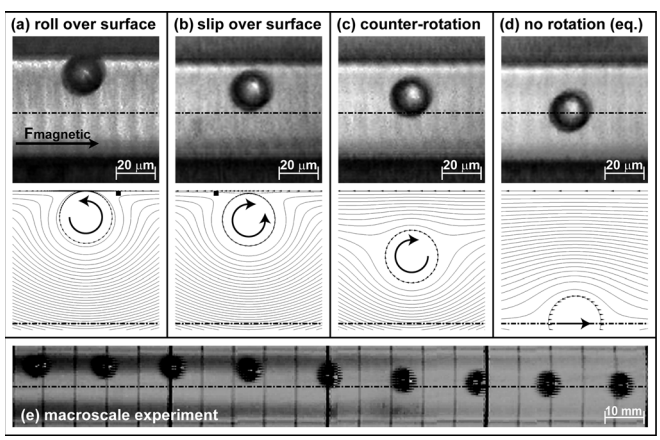

FIG. 2. Pictures of an actuated magnetic particle (20 μm, Spherotech, USA) that travels through a microchannel (100 μm diameter, 5 mm length). At the channel wall (a), the particle rolls over the surface (co-rotation). When the particle releases from the wall, it slips (b), reverses to counter-rotation (c), and focuses onto the channel center (d). A gravitation-driven experiment has been performed on the macro scale, which also shows an S-shaped trajectory curve with counter-rotation (e).

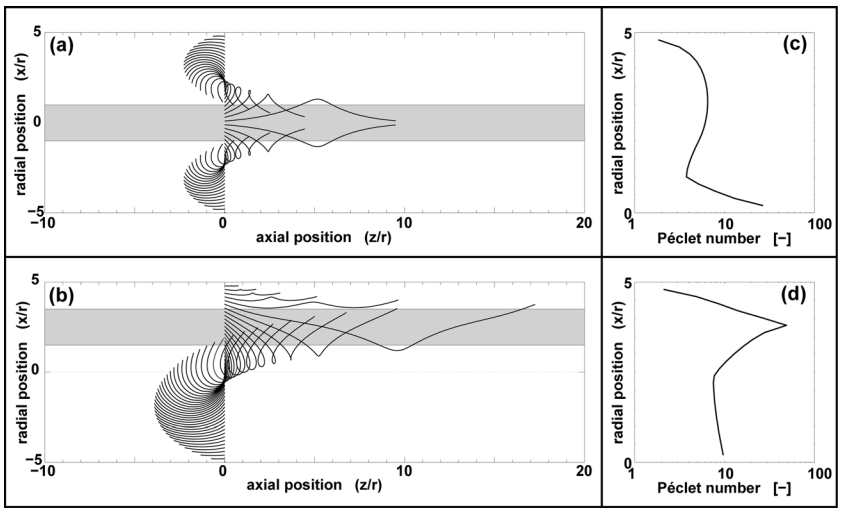

FIG. 3. Simulations of the fluid motion induced by an actuated particle (a and b) and the Péclet number (c and d) in a microchannel with radius $R=5r$. The shaded area indicates the travel path of the particle, and the lines indicate the motion of fluid elements initially distributed over the line $z=0$. Panels a and c refer to a particle that travels in the center of a channel and has no rotation. In that case, the fluid is mainly disturbed along and around the channel axis. Panels b and d refer to a particle that travels halfway between the wall and the center ($x=0.5R$). The particle will counter rotate and mainly disturb fluid volumes in the vicinity of the particle and the wall.

without any slip, as evidenced by $(\omega r)/v=-1$. Subsequently, the passive particle slowly decreases its co-rotation until it stops rotating: $(\omega r)/v=0$. The actuated particle, however, changes its rotation direction once it is released from the wall and starts to counter rotate reaching a maximum of $(\omega r_p)/v_p=+0.5$. When it approaches the channel center, the counter-rotation velocity vanishes, $(\omega r_p)/v_p=0$.

In order to visualize the momentum transfer and fluid mixing effects, the simulation model was used to track fluid elements (initially evenly distributed on a line element from $x=-R$ to $x=R$, at $z=0$) while a particle passes by. The travel of the actuated particle starts before this line at $z=-10r$ and continues in the axial direction until no further effect is induced on the fluid elements (for this case determined at $z=20r$). The particle travel is indicated with the gray area, and the fluid trajectory lines are plotted as solid lines. As in the previous simulations, a channel radius of $R=5r$ and a length of $L=100r$ are used. In Figure 3(a), fluid trajectory lines are calculated for an actuated nonrotating particle that travels exactly through the center of the channel. Near the channel axis, most of the fluid is driven in axial direction, inducing a net fluid outflow.[2] The particle motion locally disturbs the fluid flow and induces a local backflow around the particle. However, close to the channel walls, almost no fluid motion is observed. Figure 3(b) shows the calculated fluid trajectory lines for a rotating particle traveling off-axis at a constant radial position $x=0.5R$. On average, the fluid trajectory lines are now up to twice as long as for a centered actuated particle (without rotation). The counter-rotation of the particle induces a high shear velocity between the particle and the wall. A comparison of the figures indicates that off-axis particles create much higher fluid exchange in both the axial and radial directions, especially in the low velocity areas near the channel walls. To give a more quantitative measure for the mixing performance for both cases, the local Péclet number for the agitated fluid elements is calculated as function of the radial position using $Pe=(v_fR)/D$. Here, v_f represents the average velocity of the fluid elements over their travel induced by the particle passing by. In view of potential biosensor applications, diffusion constant values D for proteins or DNA molecules ($D=10^{-11}$ m^2/s) are used in the following. The Péclet numbers are calculated as function of the radial position within the channel. Péclet values $Pe>1$ indicate convection dominated mixing. The actuated particle traveling on-axis induces advection dominated mixing especially around the center of the channel as shown in Figure 3(c). The actuated particle traveling off-axis at $x=0.5R$ induces advection dominated mixing in areas much closer to the channel wall surface, shown in Figure 3(d).

As shown, actuated particles could be supportive for pumping and mixing of fluids and biological material such as DNA or proteins in biosensor systems. To enhance sensitivity and speed in integrated high-surface-area elements, near-surface mixing can be drastically improved by actuated counter-rotating particles traveling off-axis. We have already shown that particles can be organized in these configurations by tuning the magnetic and hydrodynamic interaction forces.[2,7] Complex off-axis multi-particle configurations will even enhance mixing and shall be investigated on system level, in order to optimize fluid driving and mixing at the same time. Future research will involve studies on controlled (rather than random) particle levitation, induced by for example micro-scaled roughness on channel walls or pulsed magnetic particle triggering orthogonal to the flow direction.[18]

[1]S. Haeberle and R. Zengerle, Lab Chip **7**, 1094 (2007).
[2]R. J. S. Derks, A. J. H. Frijns, M. W. J. Prins, and A. Dietzel, Microfluid. Nanofluid. **9**, 357 (2010).
[3]D. J. Laser and J. G. Santiago, J. Micromech. Microeng. **14**, 35 (2004).
[4]J. M. Ottino and S. Wiggins, Philos. Trans. R. Soc. London A. **362**, 923 (2004).
[5]H. P. Jennissen, Phys. Fluid. **17**, 100616 (2005).
[6]N. T. Nguyen and Z. Wu, J. Micromech. Microeng. **15**, 1 (2005).
[7]R. J. S. Derks, A. J. H. Frijns, M. W. J. Prins, and A. Dietzel, Appl. Phys. Lett. **92**, 024104 (2008).
[8]G. Segré and A. Silberberg, Nature **189**, 209 (1961).
[9]P. G. Saffman, J. Fluid. Mech. **22**, 385 (1965).
[10]D. D. Joseph and D. Ocando, J. Fluid. Mech. **454**, 263 (2002).
[11]R. G. Watts and R. Ferrer, Am. J. Phys. **55**, 40 (1987).
[12]S. I. Rubinow and J. B. Keller, J. Fluid. Mech. **11**, 447 (1961).
[13]H. A. Stone, J. Fluid Mech. **409**, 165 (2000).
[14]L. E. Becker, G. H. McKinley and H. A. Stone, J. Non-Newton Fluid. Mech. **63**, 201 (1996).
[15]H. Lamb, *Hydrodynamics* (Dover, New York, 1945).
[16]COMSOL MULTIPHYSICS, v3.4.0.248 (2007).
[17]Y. J. Lui, J. Nelson, J. Feng, and D. D. Joseph, J. Non-Newton Fluid. Mech. **50**, 30 (1993).
[18]S. Van Pelt, R. J. S. Derks, M. Matteucci, M.F. Hansen, and A. Dietzel, Biomed. Microdevices **13**, 353 (2011).